Toward Tunable Band Gap and Tunable Dirac Point in Bilayer Graphene with Molecular Doping

ARTICLE *in* NANO LETTERS · NOVEMBER 2011

Impact Factor: 13.59 · DOI: 10.1021/nl2025739 · Source: PubMed

5 AUTHORS, INCLUDING:

Young Hee Lee
Sungkyunkwan University
630 PUBLICATIONS **24,025** CITATIONS
SEE PROFILE

Xiangfeng Duan
University of California, Los Angeles
173 PUBLICATIONS **18,043** CITATIONS
SEE PROFILE

NANO LETTERS

LETTER

pubs.acs.org/NanoLett

Toward Tunable Band Gap and Tunable Dirac Point in Bilayer Graphene with Molecular Doping

Woo Jong Yu,[†] Lei Liao,[†] Sang Hoon Chae,[§] Young Hee Lee,[§] and Xiangfeng Duan*[,†,‡]

[†]Department of Chemistry and Biochemistry and [‡]California Nanosystems Institute, University of California, Los Angeles, California 90095, United States

[§]Department of Energy Science, BK21 Physics Division, Sungkyunkwan University, Suwon 440-746, South Korea

ABSTRACT: The bilayer graphene has attracted considerable attention for potential applications in future electronics and optoelectronics because of the feasibility to tune its band gap with a vertical displacement field to break the inversion symmetry. Surface chemical doping in bilayer graphene can induce an additional offset voltage to fundamentally affect the vertical displacement field and the band gap opening in bilayer graphene. In this study, we investigate the effect of chemical molecular doping on band gap opening in bilayer graphene devices with single or dual gate modulation. Chemical doping with benzyl viologen molecules modulates the displacement field to allow the opening of a transport band gap and the increase of the on/off ratio in the bilayer graphene transistors. Additionally, Fermi energy level in the opened gap can be rationally controlled by the amount of molecular doping to obtain bilayer graphene transistors with tunable Dirac points, which can be readily configured into functional devices, such as complementary inverters.

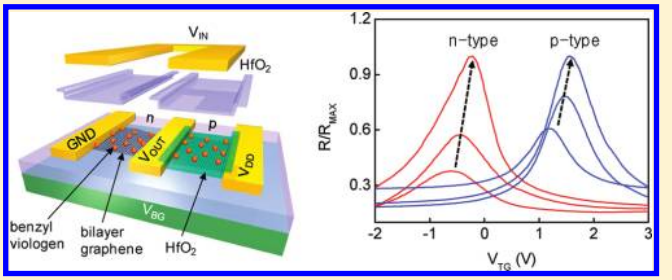

KEYWORDS: Graphene transistor, bilayer graphene, molecular doping, viologen, complementary inverter

Graphene is of considerable interest as a new electronic material for both fundamental investigations and potential applications due to its unique electronic properties, including the exceptionally high carrier mobility and carrier saturation velocity.[1−5] However, pristine graphene is a semimetal with zero bandgap and cannot be used for field effect transistors (FETs) with sufficient on/off ratio for digital electronic or photonic applications.[6−8] A number of strategies have been proposed to create a bandgap in mono- or bilayer graphenes, such as lateral quantum confinement[9,10] and breaking the inversion symmetry in bilayer graphene.[11−19] Both theoretical and experimental studies have demonstrated that a lateral confinement can be achieved in graphene nanoribbons or nanomeshes, to open up a transport band gap inversely proportional to the conducting channel width.[20−23] However, a sizable gap can only be achieved at extremely narrow channel width (typically <10 nm), which not only poses a serious technical challenge for conventional semiconductor processing but also causes severe degradation of the carrier mobility due to edge scattering effect.[24−27]

Bilayer graphene also has a gapless band structure. Interestingly, theoretical studies have suggested that a band gap can be opened in the Bernal-stacking (AB-stacking) bilayer graphene by applying an external electric filed normal to the graphene plane.[12,28,29] This theoretical prediction has recently been experimentally verified in by optical measurements[6,18,19] Electrical measurements have also demonstrated the opening of a transport gap in the bilayer graphene with vertical displacement field.[6,14−17] In particular, bilayer graphene FETs with on/off ratio up to 100 have been achieved in bilayer graphene devices at the room temperature,[30] opening the promise for logic electronics. However, the high on/off ratio in such bilayer graphene devices is often achieved only with high voltage applied to both the top and bottom gates, and the Dirac point for the maximum on/off ratio state is not controlled and usually occurs at a high-bias point due to the fundamental requirement of large vertical displacement field. On the other hand, to apply such a bilayer graphene device for possible complementary logic electronic applications, the control of the Dirac point is an import problem to address. Here we report the application of chemical molecular doping in bilayer graphene that can create an effective offset voltage not only to give rise to an additional displacement field for band gap opening but also to shift the Fermi energy level for tunable Dirac points. Threshold (Dirac point) split is demonstrated to achieve both n- and p-type bilayer graphene FETs for the construction of complementary inverters.

Figure 1a shows a schematic illustration of a dual gate bilayer graphene FET with surface molecular dopants. Reduced benzyl viologen molecules (BV) (Figure 1b) are used as the dopants to control the surface doping effect in graphene. BV is known as an n-type dopant for carbon nanotubes (CNTs)[31] because of its lower reduction potential (−1.12 V) than that of CNTs (∼0.23 V) to allow electron transfer from BV to CNTs. Similarly, coupling BV with graphene (with a reduction potential of ∼0.22 V)[32] can also result in an n-type doping effect. To fabricate the device, bilayer graphene was exfoliated from natural graphite

Received: July 27, 2011
Revised: September 25, 2011
Published: October 10, 2011

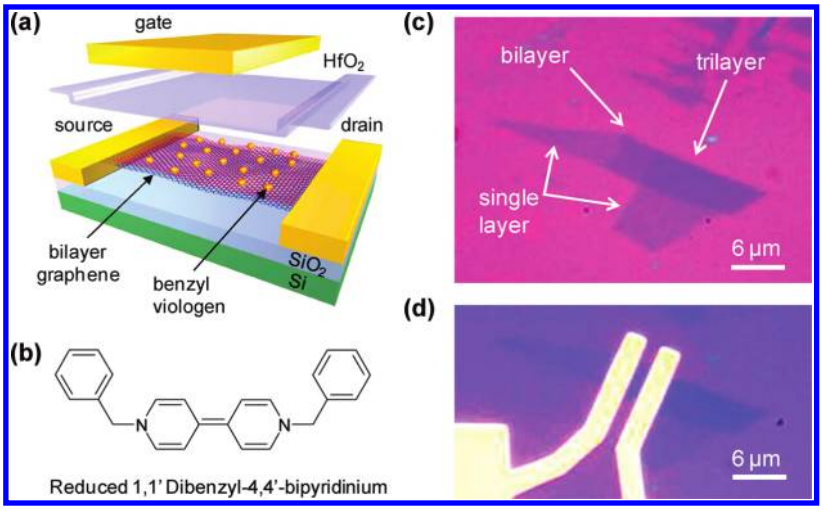

Figure 1. (a) Schematic illustration of the benzyl viologen-doped bilayer graphene dual gate transistor. From top to bottom: top gate electrode (Cr/Au), top gate dielectric (50 nm of HfO_2), benzyl viologen-doped bilayer graphene with source and drain electrodes (Cr/Au), 300 nm of SiO_2 bottom gate oxide and silicon bottom gate. (b) Molecular structure of the reduced benzyl viologen molecule. (c) Optical microscopy images of an exfoliated graphene flake and (d) the corresponding bilayer graphene FET. Arrows in (c) indicate single layer, bilayer, and trilayer graphene sheets.

and transferred onto a silicon substrate with a 300 nm silicon oxide layer. The bilayer graphene was identified based on their optical contrast (Figure 1c) and confirmed with Raman spectroscopic studies.[33] The source and drain electrodes (5 nm Cr/60 nm Au) were defined using conventional electron beam lithography process followed by a thermal evaporation metallization process (Figure 1d). The BV molecular doping was applied by spin coating a toluene solution of the reduced BV onto the substrate followed by a hot plate baking process at 100 °C for 1 min. The amount of dopants can be controlled by the number of successive spin coating processes.

The unintentionally doped graphene typically exhibits a p-type transistor characteristic with a highly positive Dirac point, likely due to an oxygen-doping effect.[34] The Dirac point can be readily tuned by applying surface molecular dopants, such as BV molecules. Electrical measurements show that the application of BV onto graphene surface produces an expected n-type doping effect to create a negative shift in Dirac points in a single bottom gated device with increasing amount of BV doping (Figure 2a).[31] The threshold voltage (Dirac point) was in the positive gate voltage regime ($\sim$ +50 V) with a p-type characteristics before BV doping (black line, Figure 2a). The threshold voltage was shifted to near the ~ -10 V, and the on/off ratio was decreased upon the first application of BV doping process (blue line, Figure 2a). The second and third applications of BV dopants further shift the threshold voltage toward increasingly negative gate voltage points (~ -37 and ~ -60 V), and the on/off ratio is also improved with increasing dopant amount (green and red lines, Figure 2a). Similar effects have also been observed recently in single bottom gated bilayer graphene devices with surface adsorbate dopants.[35]

The above observations can be explained by displacement equations. In a typical dual gate device with both the top and bottom gates, the top displacement field (D_t) and bottom displacement field (D_b) are produced by applying dual gate bias. The average of the two displacement field, $\overline{D} = (D_b + D_t)/2$, breaks the inversion symmetry of the bilayer graphene and generates a nonzero band gap.[6] The deference of the two displacement field, $\delta D = D_b - D_t$, shifts the Fermi energy (E_F)

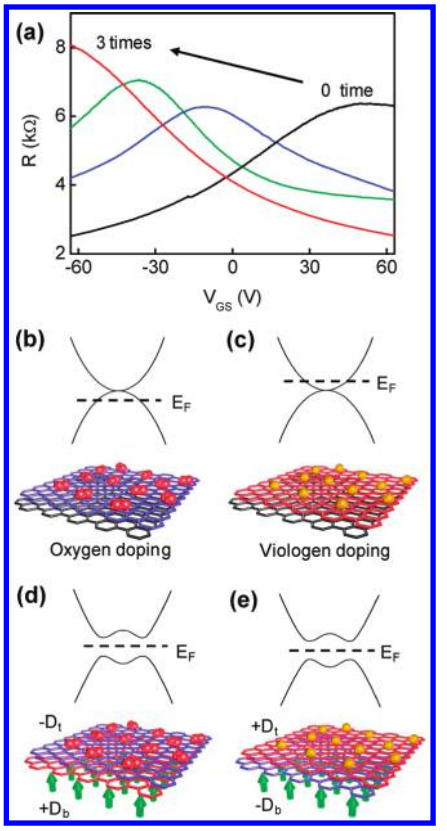

Figure 2. (a) Switching behavior as a function of bottom gate voltage with various benzyl viologen-doping amounts in a single bottom gated bilayer graphene device. Energy band structure and doping schematics of of bilayer graphene with (b) top layer p-doped by oxygen, (c) top layer n-doped by benzyl viologen, (d) additional bottom layer n-doped by a positive bottom gate voltage, and (e) additional bottom layer p-doped by a negative bottom gate voltage.

and creates a net carrier doping. At the point of $\delta D = 0$ called 'charge neutral points' (CNPs, also known as Dirac point in graphene), Fermi level is located at the middle of the conduction

dx.doi.org/10.1021/nl2025739 |*Nano Lett.* 2011, 11, 4759–4763

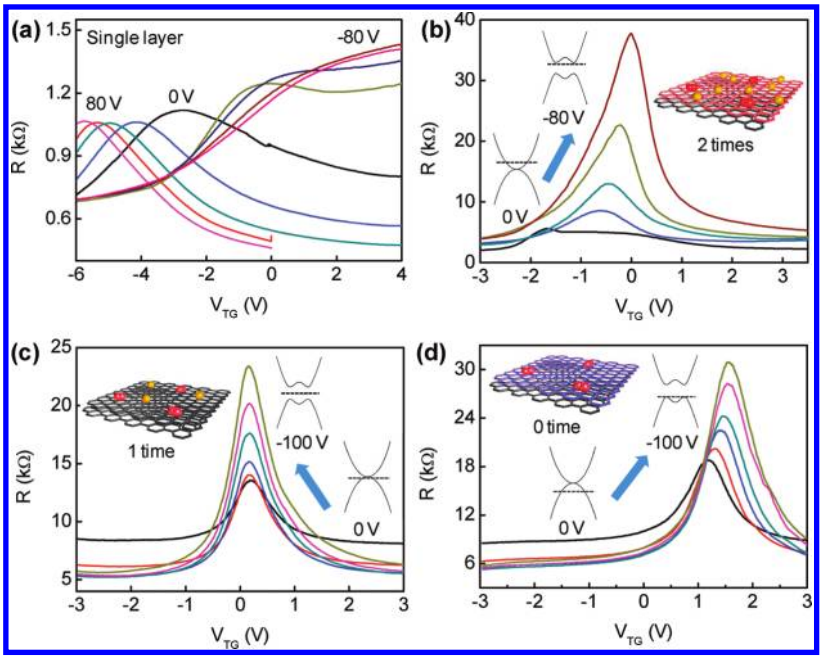

Figure 3. (a) Dual gate switching characteristics of a single layer graphene FET as a function of top gate voltage at different fixed bottom gate voltages. (b–d) Dual gate switching characteristics of bilayer graphene FET with (b) 2, (c) 1, and (d) 0 time applications of benzyl viologen doping on graphene. Bottom gate modulation steps are 20 V. Insets in (b–d) show the schematics of doping and the corresponding energy band structures before and after band gap opening.

and valence band edges, and the resistance is maximized. In general, displacement field (D) can be described using the relationship: $D_b = +\varepsilon_b(V_b - V_b^0)/d_b$ and $D_t = +\varepsilon_t(V_t - V_t^0)/d_t$, which show that the displacement field is tuned not only by the gate voltages (V_t and V_b) but also by the effective offset voltages (V_b^0 and V_t^0) which are produced by chemical dopants. Here ε and d are the dielectric constant and thickness of the dielectric layer. Since the surface molecular doping (by the BV molecules or oxygen molecules) predominantly affects the top layer of bilayer graphene, the effective offset voltage (V_t^0) of top layer is changed, and effective offset voltage (V_b^0) of bottom layer largely keeps a constant charge doping during the chemical doping process, neglecting spontaneous transfer of charges between two layers. In this way, the molecular dopants themselves induce a top layer effective offset voltage (V_t^0) to produce the total top displacement field (D_t) without an actual top gate. In Figure 2a, the Dirac point of the device without intentional molecular doping is +50 V (due to unintentional oxygen doping effect from the environment), corresponding to $D_b \approx 0.65$ V nm^{-1} considering $\varepsilon_b = 3.9$ and $d_b =$ 300 nm for thermal SiO_2. Because two displacement fields have same value ($D_b = D_t$) at the Dirac point, the top displacement field is $D_t \approx 0.65$ V nm^{-1}. With increasing BV doping, the Dirac point changed to −10, −37, and −60 V, and the corresponding top displacement field D_t changed to the −0.13, −0.48, and −0.78 V nm^{-1}, respectively.

In this way, before BV doping, oxygen doping produces a positive displacement field $D_t \approx 0.65$ V nm^{-1} with a Fermi level located at lower valence band (Figure 2b) and the corresponding threshold voltage (Dirac point) located in the positive voltage regime (Figure 2a). With increasing BV doping, the top displacement fields (D_t) are changed to −0.13, −0.48, and −0.78 V nm^{-1} for 1–3 times of doping processes, respectively. The corresponding Fermi level moves upward (Figure 2c), and the threshold voltage moves to a negative gate voltage regime (Figure 2a). The band gap is tuned by the amount of displacement field. The averages of the two displacement field ($\overline{D}$) at the Dirac point are 0.65, −0.13, −0.481, and −0.78 V nm^{-1} with 0–3 times of doping processes, respectively. Before doping, the top displacement field produced by oxygen doping along with bottom displacement filed by produced by the bottom gate voltage breaks the inversion symmetry of the bilayer to create a nonzero band gap (Figure 2d). At the first doping process, hole carriers from oxygen are neutralized by electrons from BV, and it reduces the top displacement field and band gap. After the second doping, the number of electron carriers increases with increasing BV doping, leading to an increase in the amplitude of the top displacement field, which together with bottom displacement field opens a finite or transport band gap in the bilayer graphene devices (Figure 2e). As a result, the on/off ratio is reduced at the first BV doping and increased after the second and third BV doping (Figure 2a).

The molecular doping effect can be readily employed to tune the Dirac points of the dual gated bilayer graphene devices (Figure 3). For the dual gate structure, the HfO_2 (50 nm) and Cr (5 nm)/Au (60 nm) thin films were deposited as the top gate dielectric and top gate electrode with an e-beam evaporation process.[36] The switching characteristics of the dual gate graphene FETs were characterized by the sweeping top gate voltage at fixed bottom gate voltages. As expected, the dual gate device made from single layer graphene shows little change in on/off ratio as the back gate voltage is changed from −80 to 80 V, with a maximum on/off ratio around 2 or so (Figure 3a). In contrast, the on/off ratio of all bilayer graphene devices is improved significantly as the back gate voltage is increased from 0 to −80 V, with a maximum on/off ratio exceeding 10 (Figure 3b–d), signifying the opening of a transport gap opening in bilayer graphene with vertical displacement field.

In order to further confirm the BV doping effect, the switching characteristics of dual gated bilayer graphene devices were

dx.doi.org/10.1021/nl2025739 |*Nano Lett.* 2011, 11, 4759–4763

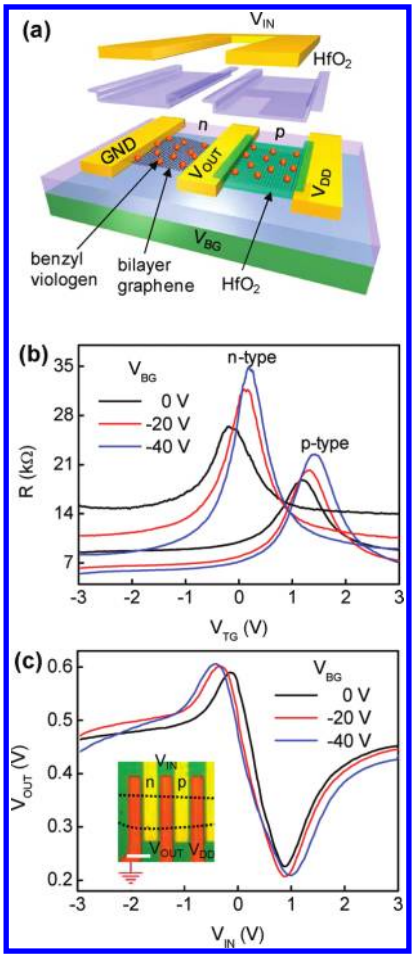

Figure 4. (a) Schematic illustration of a complementary inverter. (b) Switching behavior of n-type (BV doped) and p-type (undoped) bilayer graphene FETs as a function of top gate voltage at different bottom gate voltages. (c) Electrical switching characteristics (at various bottom-gate voltages) of a complementary inverter assembled by connecting a n- and a p-type bilayer graphene FET together. Inset shows an optical image of a complementary bilayer graphene inverter. Scale bar is 5 μm.

studied with variable doping amounts (Figure 3b−d). Without applying bottom gate voltage, the initial threshold voltages (Dirac points) of the top-gated devices with 2, 1, and 0 times of doping processes were −1, 0.15, and 1.18 V, respectively. After applying a negative bottom gate voltage to open the transport gap and achieve improved on/off ratio, the threshold voltages were changed to −0.01, 0.17, and 1.56 V for the device with 2, 1, and 0 times of doping processes, respectively. With increasing the BV doping amount, the top gate Dirac points shift toward the negative voltage direction, suggesting the upward shift of the Fermi level from the lower valence band to the upper conduction band with increasing net electron doping (insets of Figure 3b−d). The application of additional negative bottom gate voltage opens the band gap and changes the net carrier doping. The on/off ratios were increased, and top gate threshold voltages were slightly shifted to the positive direction as well. The threshold voltage differences achieved in devices with different doping amount were largely retained during the dual gate modulation and gap opening process.

The ability to achieve high on/off ratio bilayer graphene devices with tunable threshold voltage (Dirac point) readily allows the construction of functional devices, such as complementary inverter using dual gated p- and n-type bilayer graphene FETs. Figure 4a illustrates the schematics of a complementary inverter constructed using both p- and n-type bilayer graphene devices fabricated on the same graphene flake. Specifically, two intrinsically p-doped graphene FETs were first fabricated on the same bilayer graphene in series, with one of the FET selectively converted into n-type using BV doping. For selective BV doping, one FET was first covered by a 10 nm HfO_2 protecting layer using an e-beam lithography and e-beam evaporation deposition process. BV molecules were then spin coated onto the substrate to render the uncovered FET n-type. Finally, the top gate dielectric (HfO_2 50 nm) and top gate electrode (Cr 5 nm/Au 60 nm) were deposited. Electrical measurements of switching characteristics of the two bilayer graphene FETs show distinct Dirac points (Figure 4b), as a result of selectively doping one FET only. As discussed above (Figure 3b−d), the on/off ratio of both p- and n-type bilayer graphene devices increases with increasing the negative back gate voltage, while the threshold voltage difference is roughly maintained. Figure 4c shows electrical switching characteristics of the complementary inverter assembled by using n- and p-type bilayer FETs. Supply voltage (V_{DD}) of 1 V was applied to the right electrode of p-type bilayer FET, and the left electrode of n-type bilayer FET was grounded. Output voltage (V_{OUT}) was measured with varying input voltage (V_{IN}). Two output voltage peaks were observed near the 0 and 1 V, around the Dirac points of the two FETs. According to the voltage division between the p- and n-type FETs, the upper peak appears near the off state of n-type FET and the lower peak shows at the off state of p-type FET. With increasing bottom gate voltage, the off resistance of each FET increases, which in turn improves the on/off ratio of inverter output voltage.

In summary, we have demonstrated that chemical molecular doping can produce an additional displacement field to facilitate the opening of a transport gap in bilayer graphene and to tune Dirac points (threshold voltage) in single and dual gated graphene FETs. Complementary inverter was assembled using bilayer graphene FETs with split thresholds. The on/off ratio of the inverter can be tuned by the perpendicular electrical field. Our study for the first time demonstrates the exciting potential in exploring the molecular doping to rationally tune the electronic properties of bilayer graphene devices for functional circuits.

AUTHOR INFORMATION

Corresponding Author

*E-mail: xduan@chem.ucla.edu.

ACKNOWLEDGMENT

We acknowledge the Nanoelectronics Research Facility (NRF) and the Center for High Frequency Electronics (CHFE) at UCLA for technical support. X.D. acknowledges support by NSF CAREER award 0956171 and by the NIH Director's New Innovator Award Program, part of the NIH Roadmap for Medical Research, through grant 1DP2OD004342-01. Y.H.L. acknowledges financial support by the STAR faculty project (2010-0029653) and WCU program (R31-2008-000-10029-0) through the KOSEF funded by the MEST.

REFERENCES

(1) Novoselov, K. S.; Geim, A. K.; Morozov, S. V.; Jiang, D.; Zhang, Y.; Dubonos, S. V.; Grigorieva, I. V.; Firsov, A. A. *Science* **2004**, *306*, 666.

(2) Novoselov, K. S.; Geim, A. K.; Morozov, S. V.; Jiang, D.; Katsnelson, M. I.; Grigorieva, I. V.; Dubonos, S. V.; Firsov, A. A. *Nature* **2005**, *438*, 197.
(3) Dean, C. R.; Young, A. F.; Meric, I.; Lee, C.; Wang, L.; Sorgenfrei, S.; Watanabe, K.; Taniguchi, T.; Kim, P.; Shepard, K. L.; Hone, J. *Nat. Nanotechnol.* **2010**, *5*, 722.
(4) Wu, Y. Q.; Lin, Y. M.; Bol, A. A.; Jenkins, K. A.; Xia, F. N.; Farmer, D. B.; Zhu, Y.; Avouris, P. *Nature* **2011**, *472*, 74.
(5) Liao, L.; Lin, Y. C.; Bao, M. Q.; Cheng, R.; Bai, J. W.; Liu, Y. A.; Qu, Y. Q.; Wang, K. L.; Huang, Y.; Duan, X. F. *Nature* **2010**, *467*, 305.
(6) Zhang, Y.; Tang, T.; Girit, C.; Hao, Z.; Martin, M. C.; Zettl, A.; Crommie, M. F.; Shen, Y. R.; Wang, F. *Nature* **2009**, *459*, 820.
(7) Wang, F.; Zhang, Y.; Tian, H.; Girit, C.; Zettl, A.; Crommie, M.; Shen, Y. R. *Science* **2008**, *320*, 206.
(8) Xia, F.; Mueller, T.; Lin, Y.-M.; Valdes-Garcia, A.; Avouris, Ph. *Nat. Nanotechnol.* **2009**, *4*, 839.
(9) Nakada, K.; Fujita, M.; Dresselhaus, G.; Dresselhaus, M. S. *Phys. Rev. B* **1996**, *54*, 17954.
(10) Wakabayashi, K.; Fujita, M.; Ajiki, H.; Sigrist, M. *Phys. Rev. B* **1999**, *59*, 8271.
(11) McCann, E.; Falko, V. *Phys. Rev. B* **2006**, *74*, 161403(R).
(12) Castro, E. V.; Novoselov, K. S.; Morozov, S. V.; Peres, N. M. R.; Lopes dos Santos, J. M. B.; Nilsson, J.; Guinea, F.; Geim, A. K.; Neto, A. H. C. *Phys. Rev. Lett.* **2007**, *99*, 216802.
(13) McCann, E.; Falko, V. *Phys. Rev. Lett.* **2006**, *96*, 086805.
(14) Zou, K.; Zhu, J. *Phys. Rev. B* **2010**, *82*, 081407.
(15) Jing, L.; Velasco, J., Jr.; Kratz, P.; Liu, G.; Bao, W.; Bockrath, M.; Lau, C. N. *Nano Lett.* **2010**, *10*, 4000.
(16) Taychatanapat, T.; Jarillo-Herrero, P. *Phys. Rev. Lett.* **2010**, *105*, 166601.
(17) Yan, J.; Fuhrer, M. S. *Nano Lett.* **2010**, *10*, 4521.
(18) Li, Z. Q.; Henriksen, E. A.; Jiang, Z.; Hao, Z.; Martin, M. C.; Kim, P.; Stormer, H. L.; Basov, D. N. *Phys. Rev. Lett.* **2009**, *102*, 037403.
(19) Zhang, L. M.; Li, Z. Q.; Basov, D. N.; Fogler, M. M. *Phys. Rev. B* **2008**, *78*, 235408.
(20) Han, M. Y.; Ozyilmaz, B.; Zhang, Y.; Kim, P. *Phys. Rev. Lett.* **2007**, *98*, 206805.
(21) Li, X.; Wang, X.; Zhang, L.; Lee, S.; Dai, H. *Science* **2008**, *319*, 1229.
(22) Chen, Z.; Lin, Y.-M.; Rooks, M. J.; Avouris, Ph. *Phys. E (Amsterdam, Neth.)* **2007**, *40*, 228.
(23) Bai, J.; Duan, X.; Huang, Y. *Nano Lett.* **2009**, *9*, 2083.
(24) Li, X.; Wang, X.; Zhang, L.; Lee, A.; Dai, H. *Science* **2008**, *319*, 1229.
(25) Bai, J.; Zhong, X.; Jiang, S.; Huang, Y.; Duan, X. *Nat. Nanotechnol.* **2010**, *5*, 190.
(26) Jiao, L.; Zhang, L.; Wang, X.; Diankov, G.; Dai, H. *Nature* **2009**, *458*, 877.
(27) Kosynkin, D. V.; Higginbotham, A. L.; Sinitskii, A.; Lomeda, J. R.; Dimiev, A.; Price, B. K.; Tour, J. M. *Nature* **2009**, *458*, 872.
(28) Gava, P.; Lazzeri, M.; Saitta, A. M.; Mauri, F. *Phys. Rev. B* **2009**, *79*, 165431.
(29) Ohta, T.; Bostwick, A.; Seyller, Th.; Horn, K.; Rotenberg, E. *Science* **2006**, *313*, 951.
(30) Xia, F.; Farmer, D. B.; Lin, Y.; Avouris, Ph *Nano Lett.* **2010**, *10*, 715.
(31) Kim, S. M.; Jang, J. H.; Kim, K. K.; Park, H. K.; Bae, J. J.; Yu, W. J.; Lee, I. H.; Kim, G.; Loc, D. D.; Kim, U. J.; Lee, E.-H.; Shin, H.-J.; Choi, J.-Y.; Lee, Y. H. *J. Am. Chem. Soc.* **2009**, *131*, 327.
(32) Kim, K. K.; Reina, A.; Shi, Y.; Park, H.; Li, L.-J.; Lee, Y. H.; Kong, J. *Nanotechnol.* **2010**, *21*, 285205.
(33) Blake, P.; Hill, E. W.; Neto, A. H. C.; Novoselov, K. S.; Jiang, D.; Yang, R.; Booth, T. J.; Geim, A. K. *Appl. Phys. Lett.* **2007**, *91*, 063124.
(34) Ryu, S.; Liu, L.; Berciaud, S.; Yu, Y.-J.; Liu, H.; Kim, P.; Flynn, G. W.; Brus, L. E. *Nano Lett.* **2010**, *10*, 4944.
(35) Szafranek, B. N.; Schall, D.; Otto, M.; Neumaier, D.; Kurz, H. *Nano Lett.* **2011**, *11*, 2640.
(36) Bai, J.; Liao, L.; Zhou, H.; Cheng, R.; Lixin, L.; Huang, Y.; Duan, X. *Nano Lett.* **2011**, *11*, 2555.